Journal of Power Sources 196 (2011) 10817–10821

Contents lists available at SciVerse ScienceDirect

Journal of Power Sources

journal homepage: www.elsevier.com/locate/jpowsour

Short communication

Modification of nanocrystalline porous films by poly(ethyleneglycol) for quasi-solid dye-sensitized solar cells

Sheng Xu*, Hao Hu, Bobby Sebo, Bolei Chen, Qidong Tai, Xingzhong Zhao*

Key Laboratory of Artificial Micro- and Nano-structures of Ministry of Education and School of Physics and Technology, Wuhan University, Wuhan 430072, China

ARTICLE INFO

Article history:
Received 11 July 2011
Received in revised form 20 August 2011
Accepted 7 September 2011
Available online 14 September 2011

Keywords:
Quasi-solid DSSCs
Atomic force microscopy
Electrochemical impedance spectroscopy
Diffusion
Photovoltage

ABSTRACT

A convenient way is experimented to reduce the amount of dye in quasi-solid DSSCs but raise open-circuit photovoltage and photocurrent density. AFM stereoscopic morphology and calculated roughness of root mean square indicates looser porous configuration is formed in the modified TiO_2 film which is beneficial for the penetration of quasi-solid electrolyte. Decreased content of sensitized dye is confirmed by UV–vis absorption spectra. Electrochemical impedance spectroscopy is employed to characterize the transport and recombination of electrons and also to assess the penetration of quasi-solid electrolyte in the porous matrix of DSSCs. Analysis of charge-transfer resistance and dc resistance of impedance of diffusion of tri-iodide reveals enhanced mobility of tri-iodide in DSSCs. Photovoltaic parameters of quasi-solid DSSCs show an increased open-circuit photovoltage due to the enlarged photoelectrode film porosity and the shift of redox level. Better penetration of quasi-solid electrolyte has a predominant advantage over the negative effect caused by lose of photocurrent, to some extent, as a result of decreased adsorbed dye. The best result of this beneficial outcome occurs when the PEG loading is 20%, giving an overall cell efficiency of 5.1%.

1. Introduction

Since O'Regan and Gratzel [1] reported the dye-sensitized nanocrystalline TiO_2 solar cell with an efficiency up to 7% in 1991, many academic and commercial researchers have shown much interest in dye-sensitized solar cells (DSSCs) for its low cost of fabrication and acceptable energy conversion efficiency. Some reporters have even risen the device conversion efficiency over 10% under standard AM 1.5 sunlight [2–7]. However, most high-conversion-efficiency DSSCs are based on liquid electrolyte which is not suitable for industrialization because the problems of leakage and volatility of the solvent. Therefore, quasi-solid or solid electrolytes, such as polymer electrolyte [8–10], organic electrolyte [11,12] have been employed in DSSCs by many researchers. In these electrolytes, mobility of ions is however lower than that of liquid electrolytes. Hence the efficient penetration of non-liquid electrolyte in nanostructured thin films, or photoelectrode has very important influence on the whole performance of the device. We proposed a method to improve the DSSCs overall conversion efficiency and reduce the amount of dye by modifying nanocrystalline porous TiO_2 thin films with PEG. Micrographs of morphologies of different photoelectrodes explored with atomic force microscopy (AFM) enabling height imaging in tapping mode to compare electrolyte penetration in these photoelectrodes. UV–vis absorption spectra were analyzed to compare the amount of dye adsorbed on the inner surface of these photoelectrodes. Photovoltaic parameters, short-circuit current density J_{sc} and open-circuit voltage V_{oc}, were also analyzed to compare the effects on overall conversion efficiency of DSSCs by adjusting the amount of PEG in TiO_2 paste. Electrochemical impedance spectroscopy (EIS) was applied to characterize the transport and recombination of electrons, and to assess the penetration of quasi-solid electrolyte in DSSCs. Charge-transfer resistance and dc resistance of impedance of diffusion of tri-iodide are discussed to evaluate the mobility of tri-iodide in the device.

2. Experimental details

2.1. Materials

TiO_2 nanoparticles (P25, 20-30 nm, BET 48 $m^2\,g^{-1}$ Degussa AG, Germany)

SiO_2 nanoparticles (aerosil 200, 12–15 nm, Degussa AG, Germany);
LiI (Acros); I_2 (Beijing Yili chemicals, China);
N719 (Solaronix, Switzerland);

* Corresponding authors. Tel.: +86 27 87642784; fax: +86 27 87642569.
E-mail addresses: sxu@whu.edu.cn (S. Xu), xzzhao@whu.edu.cn (X. Zhao).

0378-7753/$ – see front matter © 2011 Elsevier B.V. All rights reserved.
doi:10.1016/j.jpowsour.2011.09.015

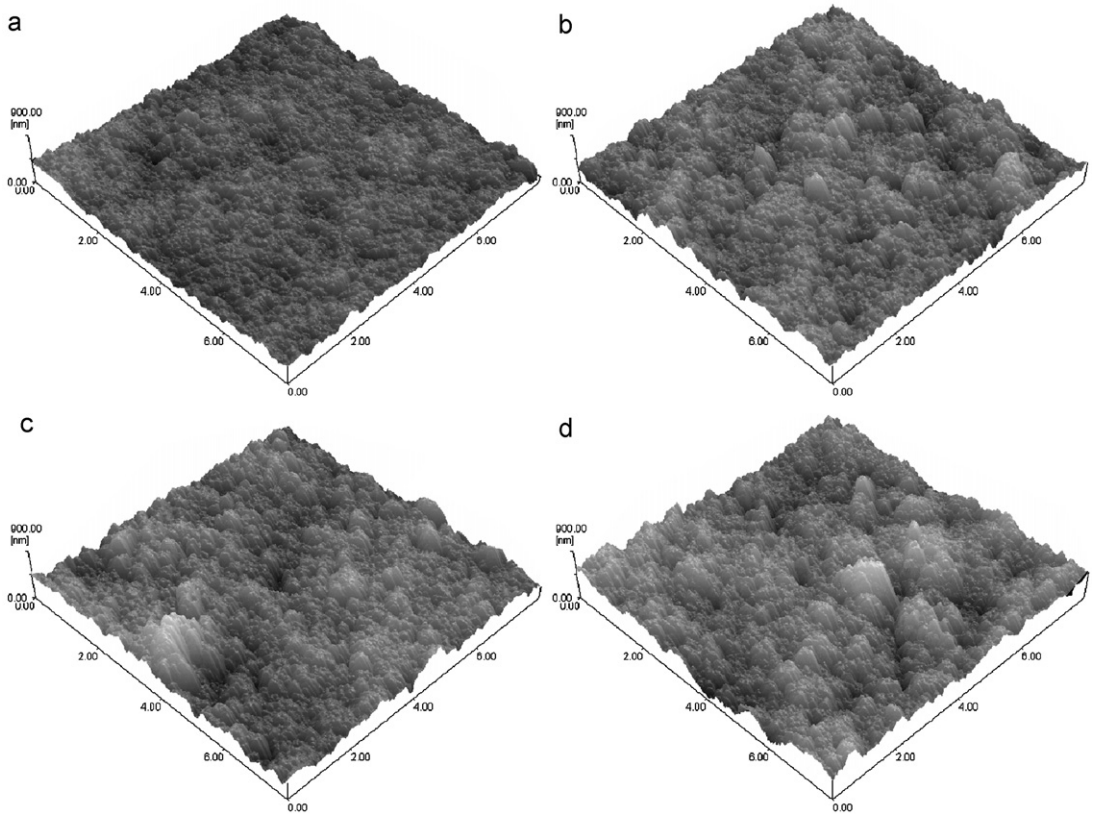

Fig. 1. Stereoscopic morphologies of different photoelectrodes: (a) 10% PEG added, (b) 20% PEG added, (c) 30% PEG added, (d) 40% PEG added in the paste scanned with AFM in tapping mode.

Triton-X100, ethanol, acetylacetone, Propylene Carbonate (PC) were purchased from Sinopharm Chemical Reagent Corporation (China);

Fluorine-doped SnO_2 conductive glass (FTO, transmission > 80% in the visible, sheet resistance 15 Ω square^{-1}, Japan);
Dodecyl-trimethoxysilane (Wuhan University, China);
PEG (poly(ethylene glycol), $M_w = 2 \times 10^4$ g mol^{-1}, Aldrich);
PEO (poly(ethylene oxide), $M_w = 2 \times 10^6$ g mol^{-1}, Aldrich);
P(VDF-HFP) (poly(vinylidenefluoride-cohexafluoropropylene), $M_w = 4.77 \times 10^5$ g mol^{-1}, Elf Atochem);

All the reagents used were of analytical purity and used without further purification.

2.2. Fabrication of dye-sensitized TiO_2 photoanode

TiO_2 nanoparticles (P25) were dispersed in 20 ml ethanol and de-ionized water with 0.8 ml acetylacetone. The amounts of 10, 20, 30 and 40% PEG (wt% of the P25 TiO_2 nanoparticles) were added each, respectively, to a separate solution prepared above. Each of the above mixture was ground in an attritor mill for 24 h, then 20 ml ethanol and 0.6 ml triton-X100 were added, and the whole content ground for additional 48 h. The prepared TiO_2 paste was spread on a transparent conducting glass with the conventional "doctor blade" technique. All TiO_2 films were sintered at 450 °C for 30 min. After cooling down to 120 °C, the TiO_2 photoanodes were immersed in the dye N719 ethanol solution and kept at 60 °C overnight to allow the dye to soak into the pores and adsorb on the surface of the TiO_2 nanoparticles. The thickness of each nanoporous TiO_2 photoelectrode obtained was 12 μm, as measured by a profilometer (Form Talysurf Profiler-S4C, Taylor Hobson, UK). The stereoscopic morphologies of the photoelectrodes, prior to dye-sensitization, were scanned by AFM (measured with a SPM-9500J3, Shimadzu, Japan) in tapping mode. The UV–visible spectroscopy of the dye-sensitized TiO_2 photoanodes was measured by a UV–vis–NIR spectrometer (cary 5000, Varian) with a wavelength ranging from 450 nm to 800 nm.

2.3. Assembly and characterization of the dye-sensitized solar cells

The polymer electrolytes were prepared according to details given in a previous report [8]. The dye-sensitized nanocrystalline TiO_2 photoelectrodes were heated in oven at 80 °C for several minutes to evaporate water from the pores of the photoelectrodes, making the electrolyte easy to penetrate into the pores of the porous photoanodes. Then the prepared electrolytes were dropped on the surface of the photoanodes and kept in the oven at 80 °C for 2 h to evaporate the redundant organic solvent. Finally, the sputtered Pt counter electrodes were pressed tightly onto the polymer electrolyte with small clips. Baking was continued till counter electrodes stuck to the photoanodes firmly.

Following assembly, several characteristics of the device were evaluated. For current–voltage characteristics measurements, a 1000 W xenon light source (Newport91192, USA) was used to simulate the solar emission (73.5 mW cm^{-2}, AM 1.5) and a Keithley 2400 digital source meter unit (USA) was used to measure the current-voltage curves under the light. The light intensity was calibrated by a Si-1787 photodiode (spectral response range: 320–730 nm). The active area of DSSCs was controlled at 0.25 cm^2 by a mask. EIS spectra were recorded over a frequency range of 10^{-2} to 10^5 Hz at room temperature. The applied bias voltage was set at open circuit voltage of the DSSCs, and the ac amplitude was 10 mV.

Table 1
The roughness calculated from AFM and the properties determined by EIS measurements of different photoelectrodes. RMS is roughness of root mean square; r_P, resistance at the Pt surface; R_k, charge-transfer resistance related to recombination of electrons; and R_D, dc resistance of impedance of diffusion of tri-iodide.

Photoelectrodes	RMS (nm)	r_P (Ω)	R_k (Ω)	R_D (Ω)
10% PEG added	59.8	2.6	34.8	12.1
20% PEG added	82.6	4.0	22.0	10.1
30% PEG added	101.8	3.6	20.9	8.0
40% PEG added	112.5	3.3	19.4	5.6

3. Results and discussion

3.1. AFM studies of TiO_2 photoelectrodes fabricated with different amounts of PEG added in the paste

In view of different amounts of PEG added in TiO_2 paste, the fabricated distinct photoelectrodes exhibit various degree of penetration. As a widely used nondestructive method, AFM was used to explore the stereoscopic morphologies and to compare the degree of compact structure of the different photoelectrodes [13]. Probing with high-resolution tapping mode AFM (Fig. 1), it was revealed that the photoelectrode fabricated with little amount of PEG (10%) presents compact porous configuration which makes it rather difficult for quasi-solid electrolyte to penetrate fully into the photoelectrode. In the case of increased amount of PEG (40%) added, the fabricated photoelectrode formed looser porous configuration which is convenient for the penetration of quasi-solid electrolyte. Roughness of root mean square (RMS) calculated from AFM reveals an obvious increase with the increase in PEG. The RMS measurements listed in Table 1 are 59.8, 82.6, 101.8 and 112.5 nm, respectively, for the cases of 10, 20, 30 and 40% of PEG added to TiO_2 pastes. This means that more amount of PEG in the TiO_2 paste leads to more incompact porous photoelectrode which enhances favorable penetration of quasi-solid electrolyte in DSSCs.

3.2. UV–vis study of TiO_2 photoelectrode films with different amounts of PEG loading in the paste

The incompact porous photoelectrode shows the advantage of better penetration of quasi-solid electrolyte, it also decreases the amount of dye sensitized onto the inner surface of the photoelectrode and consequently decreases the number of photon-excited electrons. UV–visible spectroscopy (Fig. 2) provides the absorption

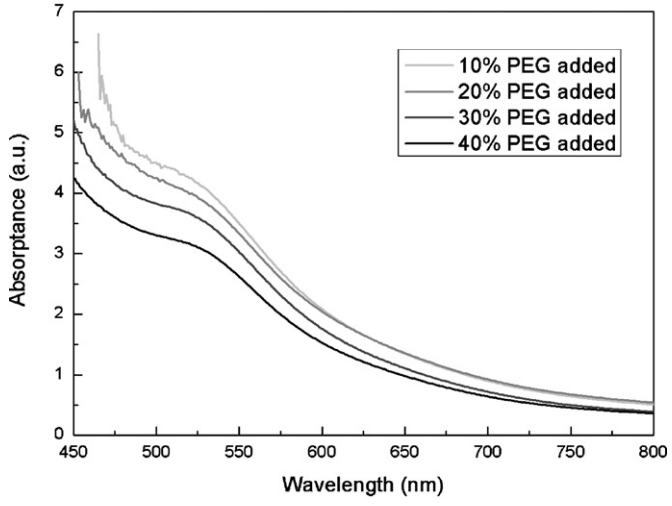

Fig. 2. Absorption spectra of N719 dyes adsorbed onto the TiO_2 photoelectrode films fabricated with different amounts of PEG in the paste.

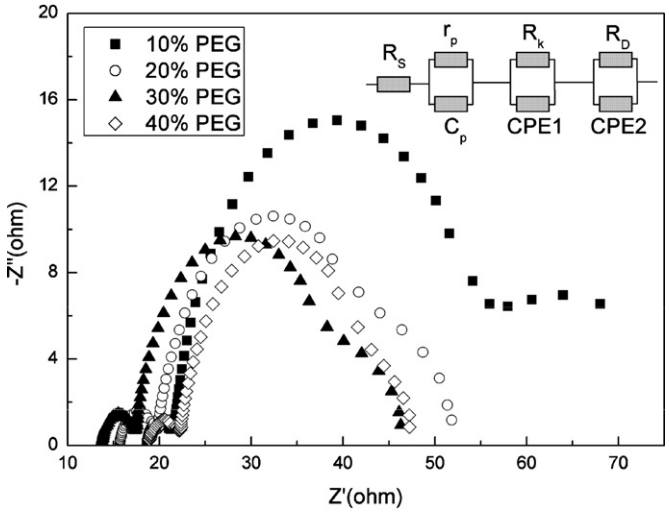

Fig. 3. Nyquist plots of the DSSC fabricated with TiO_2 photoelectrode films with different contents of PEG in the paste.

spectra of dyed photoelectrodes which were fabricated with different amounts of PEG. The peak around 535 nm is ascribed to the absorption of dye N-719 [14,15]. In the case of the paste with 10% PEG, the absorption intensity is obviously higher than others since most of the absorption is concentrated in the shortwave region of the visible light for N-719. The absorption intensity decreases as the amount of PEG in the TiO_2 paste increases. This trend shows that looser configuration of photoelectrode fabricated with a large amount of PEG in paste loses the benefit of forming larger inner surface area, an essential property which determines the amount of dye sensitized of the photoelectrodes. This result inevitably hampers photocurrent density in some way.

3.3. EIS analysis of DSSCs fabricated with photoelectrodes of different PEG loadings to paste

Kern et al. and Bisquert, respectively, reported an analysis of EIS which describes electron transport and charge recombination in DSSCs [16–18]. It is well established that the response in the high frequency part is associated with the charge transfer at the counter electrode; while the intermediate frequency part is related to the electron transport in the porous TiO_2 film and recombination at the TiO_2/electrolyte interface; and the low frequency region is attributed to the diffusion in the electrolyte. From EIS Fig. 3, the diameter of the low frequency arc, which indicates the dc resistance of impedance of diffusion of tri-iodide R_D, decreased from 12.1 Ω in the case of 10% PEG to 10.1, 8.0, and 5.6 Ω, respectively, in the cases of 20, 30 and 40% PEG content, as presented in Table 1. The decrease of dc resistance of impedance of diffusion implies enhanced mobility of tri-iodide in the DSSCs. It also confirms the enhanced penetration of quasi-solid electrolyte as a result of increased PEG loading in the TiO_2 paste. Since the diameter of the high frequency arc, which represents the resistance at the Pt surface r_P, is about 3 Ω for all the cases, the different photoelectrodes fabricated relating to different PEG contents in the paste did not show apparent effect on r_P. The most important part in the whole energy conversion efficiency of DSSCs associates with the intermediate frequency region seen in Fig. 3. The diameter of the central arc relates to electron transport resistance R_w in TiO_2 and charge-transfer resistance R_k which occurs due to recombination between the tri-iodide and the electron. Usually, the recombination process is much slower than the process of electron transportation through the TiO_2 layer in DSSCs, so the diameter of the central arc represents the value of R_k in the case where $R_k \gg R_w$ [19,20]. R_k decreased

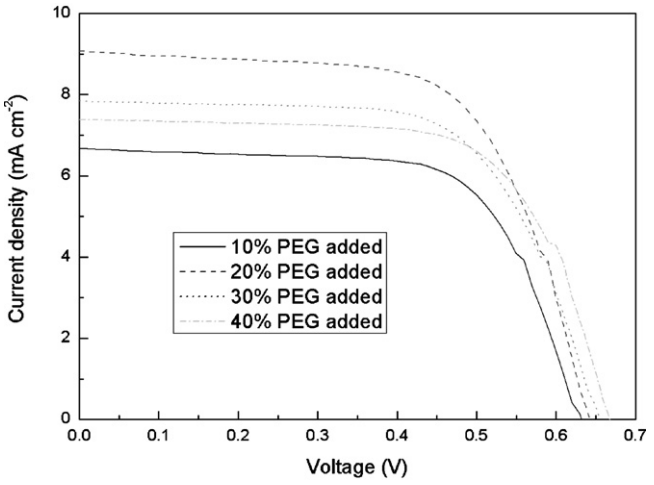

Fig. 4. Current density–voltage characteristics of DSSCs fabricated with different photoelectrodes. Measured under AM 1.5, 73.5 mW cm^{-2} light intensity, the effective DSSC area was controlled at 0.25 cm^2 by a mask.

apparently when the amount of PEG added was increased. This obviously results from the recombination between the electrons and tri-iodide. Especially in the cases of 10 and 20% PEG added, R_k evidently decreased from 34.8 Ω to 22.0 Ω (see Table 1), thus indicating the improvement of better penetration of quasi-solid electrolyte into the photoelectrodes of DSSCs without losing most part of dye adsorbed in the TiO_2 layer. Thereafter, further increase in PEG loading did not effect a significant decrease in R_k as revealed in the cases of 30 (20.9 Ω) and 40% (19.4 Ω) PEG content. The reason is that the amount of dye adsorbed onto the inner surface of the photoelectrode reduced as the amount of PEG content increased for the same electrode thickness. Decreasing the amount of dye adsorbed results in decreasing the number of photon-excited electrons, thus restricting the upward trend of recombination resulted from better penetration of electrolyte.

3.4. Photocurrent density/voltage characteristics of DSSCs fabricated with TiO_2 photoelectrode films with different amounts of PEG loading

The photocurrent density–voltage curves of DSSCs are shown in Fig. 4. The photoelectric conversion efficiencies (η) of the device fabricated with different TiO_2 photoelectrodes and their photovoltaic parameters are presented in Table 2. It is clear that open-circuit photovoltage rose from 630 to 670 mV with the amount of PEG increased from 10 to 40% in the TiO_2 paste. The open-circuit photovoltage is determined by the difference between the quasi-Fermi level of electrons in TiO_2 under illumination and the redox potential of the electrolyte [21]. The reduced amount of dye adsorbed onto the inner surface of the photoelectrode and the better penetration of quasi-solid electrolyte have opposing contributions to the photoinjected electron density, so that their effects on the open-circuit photovoltage countervail to some extent. The photoaccumulated charge in the TiO_2 film can be converted to electron concentration (n) by the expression [22]

$$n = \frac{q\varphi I_0 \tau}{q(1-P)d} \quad (1)$$

where q is the charge of an electron, φ is the ratio of injected electrons to incident photons, I_0 is the incident photon flux density or incident light intensity, τ is time constant, P is a film porosity and d is the thickness of TiO_2 photoelectrode film. Since the photoelectrode film porosity is enlarged with increase of PEG content, increased electron density n caused a negative potential shift of the quasi-Fermi level under illumination. Otherwise, V_{oc} depends logarithmically on the inverse concentration of I_3^- under illumination [19,23]. The expression for the redox potential with respect to the iodide/iodine concentrations is

$$E = E^0 + \frac{kT}{2q}\ \mathrm{Ln}\ \frac{[I_3^-]}{[I^-]^3} \quad (2)$$

where E^0 is standard potential, k is the Boltzman constant, and T is the temperature. Convenient penetration of quasi-solid electrolyte reduced the concentration I_3^- accumulated and resulted in positive potential shift of redox potential. So the V_{oc} increased obviously as we expected. Accompanied with the amount of PEG increase in the TiO_2 paste are the consequent reduction of dye adsorbed onto the inner surface of the photoelectrode and better penetration of quasi-solid electrolyte, and these two outcomes have contrary effects on the photocurrent. Poor penetration of quasi-solid electrolyte in the DSSCs caused the lowest photocurrent density even when the amount of adsorbed dye was the largest in the case of 10% PEG loading as compared to other PEG loadings in the TiO_2 paste. For the case of 20% PEG added in the TiO_2 paste in the range of our experiments, the effect of better penetration of the electrolyte predominated, resulting in the highest photocurrent. At this PEG concentration level, 5.1% energy conversion efficiency was attained. Reduced amount of dye adsorbed onto the inner surface of the photoelectrode gradually caused a decrease in photocurrent and thus retarded the favorable effect of penetration of the electrolyte. At higher amounts of PEG concentration, such as 30% and 40%, the negative effect due to reduced dye outweighs the positive effect generated by increase electrolyte penetration. The energy conversion efficiency consequently decreased to 4.5% for both cases of 30% and 40% PEG loadings, while for the case of 10% PEG, the energy conversion efficiency dropped further to 3.8%.

Table 2
The photovoltaic parameters of DSSC photoelectrodes fabricated with different amounts of PEG added in the paste. J_{sc}, short-circuit density; V_{oc}, open-circuit voltage; FF, fill factor; η, photovoltaic conversion efficiency.

DSSCs fabricated with photoelectrodes	J_{sc} (mA cm^{-2})	V_{oc} (mV)	FF	η (%)
10% PEG added	6.7	630	0.67	3.8
20% PEG added	9.1	640	0.64	5.1
30% PEG added	7.9	660	0.64	4.5
40% PEG added	7.4	670	0.67	4.5

4. Conclusions

We demonstrated a convenient method of adding PEG in TiO_2 paste to reduce the amount of dye adsorbed onto the inner surface of the photoelectrode in DSSCs but raise the open-circuit photovoltage and the photocurrent density concurrently. AFM stereoscopic morphology reveals that the photoelectrode of DSSCs fabricated with a higher amount of PEG in the TiO_2 paste form looser porous configuration, which is convenient for penetration of quasi-solid electrolyte. RMS calculated from AFM shows an obvious increase with increasing quantity of PEG. The amount of dye sensitized onto the inner surface of the photoelectrode decreased directly as the amount of PEG increased in the TiO_2 paste as confirmed by UV–vis absorption spectra. EIS revealed that charge-transfer resistance evidently decreased which indicates the improvement of better penetration of quasi-solid electrolyte into the photoelectrodes. And the decrease of dc resistance of impedance of diffusion of tri-iodide characterized by EIS indicates enhanced mobility of tri-iodide in the DSSCs. Photovoltaic parameters of the fabricated DSSCs indicate that raised open-circuit photovoltage is caused by enlarged photoelectrode film porosity and the shift of redox level.

Better penetration of quasi-solid electrolyte predominant advantaged effect on the photocurrent for the case of 20% PEG content in TiO_2 paste, giving an energy conversion efficiency of 5.1%. Finally, we conclude that varying the percentage of PEG loading in TiO_2 to fabricate photoelectrodes is beneficial for quasi-solid or solid electrolytes in DSSCS applications. Also, we suggest that employing different molecular weights of PEG might have correspondingly different effects on DSSCs.

Acknowledgments

We gratefully acknowledge the financial support of this work by the National Basic Research Program (no. 2011CB933300) of China and the National Science Fund for Talent Training in Basic Science (grant no J0830310).

References

[1] B. O'regan, M. Gratzel, Nature 353 (1991) 737.
[2] M.K. Nazeeruddin, P. Pechy, T. Renouard, S.M. Zakeeruddin, R. Humphry-Baker, P. Comte, P. Liska, L. Cevey, E. Costa, V. Shklover, L. Spiccia, G.B. Deacon, C.A. Bignozzi, M. Gratzel, Am. Chem. Soc. 123 (2001) 1613.
[3] L.Y. Han, N. Koide, Y. Chiba, A. Islam, R. Komiya, N. Fuke, A. Fukui, R. Yamanaka, Appl. Phys. Lett. 86 (2005) 213501.
[4] Y. Chiba, A. Islam, R. Komiya, N. Koide, L.Y. Han, Appl. Phys. Lett. 88 (2006) 223505.
[5] L.Y. Han, N. Koide, Y. Chiba, A. Islam, T.C Mitate, Rev. Chim. 9 (2006) 645–651.
[6] N. Koide, A. Islam, Y. Chiba, L.Y. Han, Photochem. Photobiol. A 182 (2006) 296.
[7] S. Ito, H. Miura, S. Uchida, M. Takata, K. Sumioka, P. Liska, P. Comte, P. Pechy, M. Graetzel, Commun. Chem. 41 (2008) 5194.
[8] J. Zhang, Y. Yang, S.J. Wu, S. Xu, C.H. Zhou, H. Hu, B.L. Chen, X.D. Xiong, B. Sebo, H.W. Han, X.Y. Zhao, Nanotechnology 19 (2008) 245202.
[9] W. Kubo, T. Kitamura, K. Hanabusa, Y. Wada, S. Yanagida, Chem. Commun. 4 (2002) 374.
[10] M.Y. Li, S.J. Feng, S.B. Fang, X.R. Xiao, X.P. Li, X.M. Zhou, Y. Lin, Electrochim. Acta 52 (2007) 4858.
[11] B. Macht, M. Turrion, A. Barkschat, P. Salvador, K. Ellmer, H. Tributsch, Sol. Energy Mater. Sol. Cells 73 (2002) 163.
[12] N. Hirata, J.E. Kroeze, T. Park, D. Jones, S.A. Haque, A.B. Holmes, J.R. Durrant, Chem. Commun. 5 (2006) 535.
[13] J.G. Chen, H.Y. Wei, K.C. Ho, Sol. Energy Mater. Sol. Cells 91 (2007) 1472.
[14] Z.S. Wang, M. Yanagida, K. Sayama, H. Sugihara, Chem. Mater. 18 (2006) 2912.
[15] J. Qu, X.P. Gao, G.R. Li, Q.W. Jiang, T.Y. Yan, Phys. Chem. C 113 (2009) 3359.
[16] R. Kern, R. Sastrawan, J. Ferber, R. Stangl, J. Luther, Electrochim. Acta 47 (2002) 4213.
[17] J. Bisquert, Phys. Chem. B 106 (2002) 325.
[18] J. Bisquert, G. Garcia-Belmonte, F. Fabregat-Santiago, P.R. Bueno, Electroanal. Chem. 475 (1999) 152.
[19] Q. Wang, J.E. Moser, M. Gratzel, J. Phys. Chem. B 109 (2005) 14945.
[20] M. Adachi, M. Sakamoto, J. Jiu, Y. Ogata, S. Isodas, J. Phys. Chem. B 110 (2006) 13872.
[21] A.J. Frank, N. Kopidakis, J. van de Lagemaat, Coord. Chem. Rev. 248 (2004) 1165.
[22] G. Schlichthorl, S. Huang, J. Sprague, A. Frank, J. Phys. Chem. B 101 (1997) 8141.
[23] M. Koelsch, S. Cassaignon, C. Ta Thanh Minh, J.F. Guillemoles, J.P. Jolivet, Thin Solid Films 451 (2004) 86.